Published in final edited form as:
Free Radic Biol Med. 2009 October 1; 47(7): 1019–1027. doi:10.1016/j.freeradbiomed.2009.07.008.

Mitochondrial dihydrolipoyl succinyltransferase deficiency accelerates amyloid pathology and memory deficit in a transgenic mouse model of amyloid deposition

Magali Dumont[a,*], **Daniel J. Ho**[a], **Noel Y. Calingasan**[a], **Hui Xu**[a,b], **Gary Gibson**[a,b], and **M. Flint Beal**[a]

[a]Weill Cornell Medical College, Department of Neurology and Neuroscience, 525 East 68th Street, New York, New York, 10065, USA

[b]Burke Medical Research Institute, 785 Mamaroneck Avenue, White Plains, New York, 10605, USA

Abstract

Mitochondrial dysfunction and oxidative stress are involved in Alzheimer's disease (AD) pathogenesis. In human AD brains, the α-ketoglutarate dehydrogenase enzyme complex activity (α-KGDHC) is reduced. KGDHC is mostly involved in NADH production. It can also participate in oxidative stress and reactive oxygen species (ROS) production. The mitochondrial dihydrolipoyl succinyltransferase enzyme (DLST) is a key subunit specific to the α-KGDHC. In cultured cells, reduction of DLST increased H_2O_2-induced ROS generation and cell death. Thus, we asked whether partial genetic deletion of DLST could accelerate the onset of AD pathogenesis, using a transgenic mouse model of amyloid deposition crossed with $DLST^{+/-}$ mice. Tg19959 mice, which carry the human amyloid precursor protein (APP) with two mutations, develop amyloid deposits and progressive behavioral abnormalities. We compared Tg19959 mice to Tg19959-$DLST^{+/-}$ littermates at 2–3 months of age, and studied the effects of DLST deficiency on amyloid deposition, spatial learning and memory, and oxidative stress. We found that α-KGDHC activity was reduced in $DLST^{+/-}$ mice. We also found that DLST deficiency increased amyloid plaque burden, Aβ oligomers and nitrotyrosine levels, and accelerated the occurrence of spatial learning and memory deficits in female Tg19959 mice. Our data suggest that α-KGDHC may be involved in AD pathogenesis through increased mitochondrial oxidative stress.

Keywords

Alzheimer's disease; mitochondria; α-ketoglutarate dehydrogenase enzyme complex; spatial learning and memory; amyloid plaques; Aβ oligomers; oxidative stress

*Corresponding author, Magali Dumont, Weill Cornell Medical College, Department of Neurology and Neuroscience, 525 East 68th Street, A578, New York, New York, 10065, USA, Phone 212 746 4818, Fax 212 746 8276, Email mad2138@med.cornell.edu.

Introduction

Alzheimer's Disease (AD) is marked by progressive memory and cognitive impairment. Accumulation of intracellular and extracellular amyloid-β peptide (Aβ) has been linked to the pathogenesis of AD. There is considerable evidence showing that the accumulation of Aβ leads to impaired mitochondrial function [1] and subsequently increased production of reactive oxygen species (ROS) [2,3]. ROS are cytotoxic, and can lead to damaged lipids, proteins, nucleic acids, and carbohydrates [4]. Increased oxidative damage has previously been reported in postmortem brains of mild cognitive impairment (MCI) and AD patients, as shown by increased 3-nitrotyrosine (3-NT), an indicator of oxidative damage mediated by peroxynitrite [5,6], and by increased 4-hydroxynonenal (4-HNE), a marker of lipid peroxidation [7,8].

In spite of evidence supporting the role of Aβ as the cause of oxidative damage, several studies revealed that oxidative stress could precede amyloid pathology. Nunomura et al. have shown that the highest increase in oxidative markers occurred at an early stage in the disease progression in human patients [9]. In transgenic mouse model of amyloid deposition, lipids and proteins modified by oxidative stress are present in brains both with and without amyloid plaques [10]. Pratico and colleagues (2001) showed that elevated levels of isoprostanes, a marker of lipid peroxidation, preceded the onset of Aβ plaque formation in Tg2576 mice [10]. In mice, other markers of oxidative damage were also increased very early in the disease pathogenesis, and kept increasing with age, such as nitrotyrosine and 4-HNE [11]. Oxidative stress has also been shown to exacerbate amyloid deposition and other hallmarks of the disease. Partial deficiency of the mitochondrial manganese superoxide dismutase (MnSOD) increased amyloid plaques in Tg19959 mice [12] and tau phosphorylation in Tg2576 mice [13]. It also accelerated the onset of behavioral abnormalities in hAPP mice [14]. In addition, the overexpression of MnSOD reduced amyloid plaques, improved memory function and protected synapses [15]. Thus, mitochondria and their role in oxidative damage in neurodegeneration are a topic of great interest.

A major link between oxidative stress and mitochondrial dysfunction is the α-ketoglutarate-dehydrogenase complex (α-KGDHC) [16]. α-KGDHC is a crucial mitochondrial enzyme complex that mediates oxidative metabolism. Its activity is reduced in brains from AD patients [17–19]. α-KGDHC is comprised of three subunits: α-ketoglutarate dehydrogenase (E1; EC 1.2.4.2), dihydrolipoyl succinyltransferase (E2; EC 2.3.1.61 or DLST), and dihydrolipoyl dehydrogenase (E3; EC 1.6.4.3). Of the three components, only E1 and E2 are specific to α-KGDHC. In frontal and temporal cortices from AD patients bearing the Swedish amyloid precursor protein (APP) mutation KM670/671NL, levels of El and E2 are diminished, whereas levels of E3 remained unchanged [20]. Recently, Karuppagounder et al. (2008) reported that in Tg19959 mice, thiamine deficiency induced oxidative stress and increased amyloid plaque deposition [21]. Therefore, we asked whether E2 or DLST could be involved in AD pathogenesis in vivo, and more precisely could accelerate the onset of AD pathogenesis.

We studied the effects of its partial genetic deletion in Tg19959 mice. Tg19959 mice overexpress the human APP with two mutations (KM670/671NL and V717F). At about 4 months of age, Tg19959 mice develop amyloid plaques in the cortex, the hippocampus and the amygdala, together with cognitive deficits [22]. In our study, we crossed Tg19959 male mice with $DLST^{+/-}$ female mice and assessed amyloid burden and behavior at 2–3 months of age, when amyloid pathology normally begins and prior to any cognitive impairment. We found that in vivo DLST deficiency reduced α-KGDHC activity. It also increased amyloid plaque burden, Aβ oligomers and nitrotyrosine levels, and accelerated the occurrence of spatial learning and memory deficits in female Tg19959 mice.

Materials and methods

Animals

Tg19959 mice were obtained from Dr. George Carlson (McLaughlin Research Institute, Great Falls, MT, USA). Tg19959 mice were constructed by injecting FVB x 129S6 F1 embryos with a cosmid insert containing human APP_{695} with two familial AD mutations (KM670/671NL and V717F), under the control of the hamster PrP promoter [23]. Heterozygous $DLST^{+/-}$ deficient mice were generated with a partial deletion of the mitochondrial dihydrolipoyl succinyltransferase enzyme (Lexicon Pharmaceuticals, The Woodlands, TX, USA).

In our study, Tg19959 males were crossbred with $DLST^{+/-}$ females. Littermates of four different genotypes were produced and identified by PCR of tail DNA: Tg19959, $DLST^{+/-}$, Tg19959-$DLST^{+/-}$, and wild-type mice. Since amyloid pathology is differentially affected by gender, we analyzed cohorts of males and females separately [24,25]. We set aside one group of males for behavioral, histopathological and biochemical analysis. We also used two cohorts of females, one for behavior and the other for histopathology and biochemistry. The animals used in our study were between 2 and 3 months of age. All experiments were approved by the Weill Cornell Medical College Institutional Animal Care and Use Committee.

α-ketoglutarate dehydrogenase activity

α-KGDHC activity was monitored as the ketoglutarate dependent conversion of NAD^+ to NADH: α-ketoglutarate + NAD^+ + CoA → succinyl CoA + CO_2 + NADH. Brain tissues were homogenized in 250 μl of KGDHC lysis buffer and α-KGDHC activity was measured as described previously [17].

Behavioral study

One week prior to behavioral testing, the experimenter handled mice every day in order to habituate them. Body weights were recorded at the end of the week.

We assessed spatial learning and memory using the Morris water maze test. An opaque basin (diameter: 120 cm; height of the wall: 60 cm) was filled with water (23°C). The water was opacified with non-toxic and odor-free white tempera paint. In order to familiarize the animals with their task, we placed each mouse on a platform (diameter: 10 cm) located in the center of the basin for 20 sec. Afterwards, we performed four consecutive trials per day over two days, during which we released the animals 3–5 cm away from the platform and allowed them to search for it for a maximum of 20 sec. In addition, mice were forced to stay on the platform for 20 sec after finding it before the experimenter removed them.

During the acquisition period, we arranged extra-maze visual cues, such as light fixtures and wall posters in the room, and submerged the hidden platform in the middle of the northwest (NW) quadrant of the pool, 1 cm beneath water level. Each day, we placed the mice next to and facing the wall of the basin in four different starting positions: north, east, south, and west respectively, corresponding to four successive trials. Latencies and total distances before reaching the platform were recorded for 5 days with a video tracking system (Ethovision 3.0, Noldus Technology, Attleborough, MA, USA). For 20 min after each trial, we put the mice in plastic holding cages filled with paper towels to keep them dry and warm. Whenever a mouse failed to reach the platform within the maximum allotted time of 60 sec, it was manually placed on the platform for 5 sec.

A probe trial was conducted 24 h after the acquisition period, in which the platform was removed from the pool. We released the mice on the north side of the maze for a single trial

of 60 sec, during which the percent time spent in the NW quadrant was measured for the first 15 sec.

Animals were tested for four trials per day over two days in the visible platform version of the Morris water maze. Each trial lasted 60 sec and was followed by a 20 min inter-trial period. In this cued version, a 13 cm pole was fixed on the platform. Mice were released from the north side on the first day and from the south side of the pool on the second day. For each trial, the cued platform was moved to a different quadrant so that the mouse could only locate it visually. Latencies and total distances before reaching the visible platform were recorded.

Tissue harvest and preparation

Deep anesthesia was induced by administration of sodium pentobarbital via intraperitoneal injection, after which mice were transcardially perfused with ice cold 0.9% sodium chloride. We removed the brains and dissected them on ice. One hemibrain was snap frozen in liquid nitrogen and stored at −80 °C for biochemical assays. The other half was post-fixed in 4% paraformaldehyde for 24 hr and stored in cryoprotectant for immunohistochemical studies.

Immunohistochemistry of Aβ1–42 deposits in the retrosplenial/motor cortex and CA1/dentate region of the hippocampus

We analyzed five sections of the cortex and the hippocampus per mouse. Each section was cut 350 μm apart, from bregma −1.06 to −1.94 for the cortex and bregma −1.34 to −2.7 for the hippocampus. Sections were pretreated with 50% formic acid for 5 min before labeling with anti-Aβ1–42 rabbit polyclonal antibody AB5078P (1:1000, Chemicon, Temecula, CA, USA). Immunostaining with AB5078P was similar to that seen with the mouse monoclonal anti-Aβ antibody 6E10 (1:1000, Covance, Emerville, CA, USA) [22]. However, 6E10 also binds APP and β-C-terminal fragments in addition to Aβ, and not surprisingly produced more background staining. Therefore, since Aβ1–42 is considered to be the most pathogenic specie, quantitation was performed with AB5078P. Immunolabeling was detected by the avidin-biotin complex peroxidase method and visualized after DAB (diaminobenzidine) incubation for 5 min (Vector, Burlingame, CA, USA).

Sections were viewed with the 10X objective on a Nikon Eclipse E600 microscope, and digital images were captured using Stereo Investigator 4.35 (Microbrightfield, Burlington, VT, USA). Quantitative analysis was performed using NIH Image 1.63 (National Institute of Health, Bethesda, MD, USA). The percent area occupied by plaques and the number of plaques per 0.75 mm^2 were calculated.

Immunohistochemistry of Aβ oligomers

Adjacent sections were treated with 90% formic acid for 5 min prior to labeling with anti-oligomer antibody A11 (1:500, Invitrogen, Carlsbad, CA, USA) [26]. Immunolabeling was detected by the avidin-biotin complex peroxidase method and visualized after DAB incubation for 5 min (Vector, Burlingame, CA, USA). Quantitative analysis of the percent area occupied by A11-immunoreactivity and the A11-immunoreactive patch number per 0.75 mm^2 was done as previously described for immunohistochemistry of Aβ1–42 deposits.

ELISA of Aβ1–42 and Aβ1–40 levels

Aβ1–42 and Aβ1–40 levels were analyzed from snap frozen brain tissues that were homogenized in 6% sodium dodecyl sulfate (SDS). Aβ1–42 and Aβ1–40 ELISAs were performed using commercial kits (Invitrogen, Carlsbad, CA, USA) following the manufacturer's instructions.

Immunohistochemistry and dot-blot of nitrotyrosine

For the immunohistochemistry, adjacent sections were labeled with rabbit anti-nitrotyrosine (1:100, Millipore, Billerica, MA, USA). Immunolabeling was detected by the avidin-biotin complex peroxidase method and visualized after DAB incubation for 5 min (Vector, Burlingame, CA, USA).

For the dot-blot analysis, snap frozen brain sections were homogenized by sonication in phosphate buffered saline (PBS) containing protease inhibitor cocktail (Complete Protease Inhibitor Cocktail tablet, Roche Diagnostics, Mannheim, Germany). Protein concentration was measured (DC Protein Measurement Kit, Bio-Rad, Hercules, CA, USA). Homogenates containing 20μg of protein were spotted on nitrocellulose membrane (4 μL for each sample). Once completely dry, the membrane was blocked in 5% non-fat dry milk/PBS-Tween 20 (PBST) for 1 hour at room temperature. HRP-conjugated secondary antibody binding was visualized with enhanced chemiluminescence. Primary antibodies and concentrations were: mouse monoclonal anti-nitrotyrosine (1:500, Alexis LLC, San Diego, CA, USA); mouse monoclonal anti-α-tubulin (1:10,000, Sigma, St. Louis, MO, USA). Films were scanned at 600 dpi, and densitometry was quantified with Scion Image 4.0.2 (Scion Corp., Frederick, MD, USA).

Statistical analysis

ANOVA was used to compare all four groups. A post-hoc Fisher's PLSD (Fisher) test was used for further comparison between two groups. When only two groups were involved in the study, two-tailed unpaired t-tests were used to compare Tg19959 mice and Tg19959-DLST$^{+/-}$ littermates (Statview 5.0.1, SAS Institute Inc., Cary, NC, USA).

Results

α-ketoglutarate dehydrogenase activity was reduced in Tg19959 mice with DLST deficiency

Since DLST is critical to the proper function of α-KGDHC, we measured the activity of α-KGDHC in our mice. We found that α-KGDHC activity was significantly lower in both DLST$^{+/-}$ and Tg19959-DLST$^{+/-}$ mice compared to wild-type and Tg19959 littermates (Figure 1; Fisher $p<0.05$).

DLST deficiency increased amyloid plaque burden and Aβ oligomers in female Tg19959 mice

In order to examine amyloid plaque burden, we stained brain sections with an Aβ1–42 antibody. In our analysis of male mice, we did not find significant differences in hippocampal plaque burden between Tg19959-DLST$^{+/-}$ mice and Tg19959 littermates (Figure 2A and B). However, we did observe a trend of increased plaque number in the cortex of Tg19959-DLST$^{+/-}$ male mice (Figure 2A; t-test $p=0.0871$), as well as percent area covered by those plaques (Figure 2B; t-test $p=0.1039$). Our analysis of female mice (figure 2E) revealed no significant differences in cortical plaque burden between Tg19959-DLST$^{+/-}$ mice and Tg19959 littermates (Figure 2C and D). However, we found a significant increase of hippocampal plaque number in Tg19959-DLST$^{+/-}$ mice compared to Tg19959 littermates (Figure 2C; t-test $p<0.05$). These same mice also displayed a significant increase in the percent area covered by plaques in the hippocampus compared to Tg19959 littermates (Figure 2D; t-test $p<0.05$).

We used the A11 antibody to label Aβ oligomers in mouse brain sections. Our results did not show any differences in A11-oligomers between Tg19959-DLST$^{+/-}$ male mice compared to Tg19959 male littermates (Figure 3A and B). In females (figure 3E), Tg19959-DLST$^{+/-}$ mice had significantly more Aβ oligomers in the cortex and the hippocampus than Tg19959 littermates, as shown by the increased number of A11-positive oligomers (Figure 3C; t-test

p=0.0339 for the cortex and p=0.036 for the hippocampus) and percent area covered by A11-positive Aβ oligomers (Figure 3D; t-test p=0.0089 for the cortex and p=0.018 for the hippocampus). Thus, DLST deficiency increased amyloid burden and Aβ oligomers in female Tg19959 mice.

DLST deficiency did not affect levels of SDS-soluble Aβ1–42 and Aβ1–40 in Tg19959 mice

Levels of 6% SDS-soluble Aβ1–42 and Aβ1–40 were assessed by ELISA. For both males and females, DLST deficiency did not change levels of SDS-soluble Aβ1–42 (Figure 4A and C) and Aβ1–40 (Figure 4B and D) in Tg19959 mice.

DLST deficiency induced spatial learning and memory impairment in female Tg19959 mice

In this section, we provided preliminary data on the effect of DLST deficiency on cognitive behavior. We had 5–8 animals per group, except for the cohort of female mice where we had only one Tg19959 mouse. We still performed the experiment and presented the results (as informative data).

Body weights were recorded prior to behavioral testing. In both genders, Tg19959 and Tg19959-DLST$^{+/-}$ mice had decreased body weights in comparison to wild-type littermates (Supplementary figure 1A and 1B, $p<0.05$). However, there was no significant difference between Tg19959 mice and Tg19959-DLST$^{+/-}$ littermates.

Spatial learning and memory were assessed using the Morris water maze test. We recorded latency and total distance before the mice reached the hidden platform during the 5-day acquisition period. Our results from the probe trial were collected from a single trial and expressed as the percent time spent in the NW quadrant during the first 15 sec. Comparison between all groups of male mice showed no significant differences for the acquisition period (Figure 5A and B) or the probe trial (Figure 5E).

However when we compared female mice during the entire acquisition period (Figure 5C and D), we found that Tg19959-DLST$^{+/-}$ mice swam longer and traveled greater distance before reaching the platform than wild-type (Fisher $p<0.05$) and DLST$^{+/-}$ mice (Fisher $p<0.05$). During the probe trial (Figure 5F), Tg19959-DLST$^{+/-}$ mice spent less time in the NW quadrant than their wild-type (Fisher p=0.0746) and DLST$^{+/-}$ littermates (Fisher $p<0.05$). Thus, our data suggest that DLST deficiency induced spatial learning and memory deficits in female Tg19959 mice compared to wild-type and DLST$^{+/-}$ littermates.

DLST deficiency did not affect performances of Tg19959 mice in the cued version of the Morris water maze (data not shown).

DLST deficiency increased nitrotyrosine levels in female Tg19959 mice

Since DLST is involved in oxidative stress, we assessed nitrotyrosine levels in wild-type, DLST$^{+/-}$, Tg19959 mice and Tg19959-DLST$^{+/-}$ littermates (figure 6AB). In males (figure 6A), there was no significant difference in nitrotyrosine brain levels. In females (figure 6BC), we observed a significant increase of nitrotyrosine levels in Tg19959 mice with DLST deficiency compared to wilt-type (Fisher, p=0.001), DLST$^{+/-}$ (Fisher, p=0.0005), and Tg19959 littermates (Fisher, p=0.0139). The difference between wild-type mice and Tg19959 littermates did not quite reach significance (Fisher, p=0.1051).

Discussion

Mitochondrial dysfunction and oxidative stress are known to play a role in Alzheimer's disease (AD) pathogenesis. In human AD brains, the mitochondrial α-ketoglutarate dehydrogenase

(α-KGDHC) activity is markedly reduced in either damaged or relatively undamaged areas [17]. These changes occur predominantly in cortical regions of the brain [18,19]. α-KGDHC is a key enzyme of the tricarboxylic acid cycle (TCA) that is composed of three subunits: a thiamine pyrophosphate-dependent dehydrogenase enzyme (E1), dihydrolipoyl succinyltransferase enzyme E2 (DLST) and dihydrolipoamide dehydrogenase enzyme (E3). Gibson et al. have previously reported that in frontal and temporal cortices from AD patients bearing the Swedish APP670/671 mutation, levels of El and DLST declined, whereas levels of E3 were unchanged [20]. It is important to note that only E1 and DLST are unique to α-KGDHC. There is a large body of evidence demonstrating that α-KGDHC and DLST participate in ROS formation and oxidative stress [16]. Thus, we asked whether DLST could accelerate the onset of AD pathogenesis in vivo by examining the effects of its partial genetic deletion in Tg19959 mice. At about 4 months of age, Tg19959 mice develop amyloid plaques in the cortex, the hippocampus and the amygdala, together with progressive cognitive deficits, as those found in TgCRND8 mice [23,27].

In our study, Tg19959 mice were crossbred with $DLST^{+/-}$ mice and offspring were tested at 2–3 months of age. At this age, amyloid pathology normally begins and cognitive impairment is not present yet (personal observations). Since, in AD pathogenesis, memory deficit is the most important clinical feature, we assessed the effects of DLST partial deficiency on spatial learning and memory in the Morris water maze. In both the acquisition period and the probe trial, which measures spatial learning and memory retention respectively, Tg19959 mice did not show any impairment in comparison with $DLST^{+/-}$ and wild-type littermates. However, Tg19959-$DLST^{+/-}$ female mice displayed spatial learning and memory retention deficits compared to wild-type and $DLST^{+/-}$ female littermates. In addition to our comparative data, we found that Tg19959-$DLST^{+/-}$ female mice were unable to learn the location of the hidden platform over the course of the acquisition period, as shown by their flat learning curve. Furthermore, they were unable to recall the location of the platform during the probe trial. Tg19959-$DLST^{+/-}$ mice spent only about 25 % of the time in the NW quadrant, which reflects a random search.

The second important pathological feature in AD is the formation of amyloid plaques. In Tg19959 mice, DLST deficiency increased amyloid plaque burden especially in female animals. In addition, we found that A11-positive Aβ oligomers were increased in the cortex and the hippocampus of Tg19959-$DLST^{+/-}$ female mice. It should be noted that the detection of Aβ oligomers is complex and highly dependent on technical factors including the antibody used. The A11 antibody is commonly used to assay Aβ oligomers, though it also recognizes oligomers of other proteins [26,28]. Taken together, these data revealed that DLST partial deficiency in vivo exacerbated AD-related phenotype mostly in female Tg19959 mice. In fact, it has been previously reported that in transgenic mouse model of amyloid deposition, female mice were affected more severely by amyloid pathology [24,25]. This gender difference could be explained by increased γ-secretase activity in aged female mice, which can lead to increased APP processing and Aβ production [29]. In our model, it is possible that the effect of DLST deficiency was enhanced by a higher APP and Aβ toxicity in females.

To further investigate the mechanism by which DLST affected AD-related phenotype, we measured levels of SDS-soluble Aβ species. Even though, there was an increase of amyloid plaques and oligomers with partial DLST deletion, levels of Aβ1–42 and Aβ1–40 were unchanged. These data suggest that partial genetic deletion of DLST could decrease resistance to Aβ toxicity. Partial DLST deficiency could also act downstream of the APP processing and Aβ production, by accelerating the rate of plaque formation and Aβ oligomerization.

There is a large body of evidence demonstrating a link between Aβ toxicity and oxidative stress. Several oxidative markers are markedly increased in transgenic mouse model of amyloid

deposition, such as protein carbonyls, nitrotyrosine and 4-HNE, even at early stage [11]. It has been shown that Aβ directly generates reactive oxygen species (ROS) in the presence of iron or copper ions [30] via methionine-35 [31]. Aβ oligomers also induce neuronal oxidative stress through N-methyl-D-aspartate receptors and calcium influx [32]. Mitochondria mediated oxidative stress can also influence Aβ toxicity. Overexpression of MnSOD increased resistance to Aβ-induced toxicity in vitro [33] and in vivo [15]. On the other hand, partial deletion of MnSOD resulted in increased amyloid pathology [12]. Recently, Karuppagounder et al. (2008) reported that in Tg19959 mice, thiamine deficiency induced oxidative stress and increased amyloid plaque deposition [21]. In cells, DLST deficiency increased ROS production after H_2O_2-induced oxidative stress [34]. Thus, we postulate that DLST deficiency could reduce resistance to APP or Aβ-induced toxicity in vivo through an increase of oxidative stress. In fact, we found that Tg19959-DLST$^{+/-}$ female mice had increased oxidative stress as shown by elevated nitrotyrosine levels as compared to Tg19959 female littermates.

The detrimental effect of DLST deficiency on oxidative stress was not seen in male mice. This gender effect could be explained by an overall higher APP and Aβ toxicity in female mice. An alternative and potentially complementary explanation for the gender effect could be a differential response towards oxidative stress and mitochondrial function. Even though there is not a clear consensus on gender effect on mitochondrial function, Ali et al. have reported that female wild-type mice had a greater increase of ROS production and a lower level of antioxidant enzymes during aging than male wild-type mice [35]. Once given a superoxide dismutase mimetic, age-induced ROS production was reduced in both genders but with more efficacy in females [35]. These results suggest that female mice may be more susceptible to mitochondrial oxidative stress, which could enhance the effect of DLST deficiency.

It should be noted that in contrast to human AD brains, we did not observe any change of α-KGDHC activity at baseline in Tg19959 mouse brains compared to wild-type mouse brains. The reasons for this difference are not certain, but there may be several potential explanations. In human AD brain, reductions in KGDHC activity are region specific [19], but in our mouse study, KGDHC activity was measured on total brain homogenates. In addition, considering that α-KGDHC is constituted by multiple copies of the three subunits, it is possible that the activity of the complex is maintained by compensatory mechanisms.

In our model, partial genetic deletion of DLST diminished the activity of α-KGDHC in both DLST$^{+/-}$ and Tg19959-DLST$^{+/-}$ mice, and the detrimental effects reported in this paper could be due to this reduction of α-KGDHC activity. However, according to Shi et al., DLST can have effects on ROS production and cell death independent of α-KGDHC activity [34]. Therefore, in our model, DLST deficiency may have had other effects besides reduction in α-KGDHC activity.

As previously mentioned, oxidative stress may promote Aβ aggregation or fibrillarization. The lipid oxidation product 4-HNE from polyunsaturated lipids is able to modify three histidine residues of Aβ by Michael addition, a reaction that causes protein misfolding and accelerates fibril formation at low protein concentrations [36]. In addition, oxidized cholesterol products can also modify Aβ by Schiff base formation and accelerate Aβ aggregation [37]. Thus, by increasing oxidative stress, partial deletion of DLST could elevate the rate of plaque formation and Aβ oligomerization. This mechanism of action has been proposed to explain the beneficial role of the mitochondrial antioxidant response in AD pathogenesis. Overexpression of manganese superoxide dismutase in Tg19959 mice reduced amyloid plaques, without affecting APP processing or Aβ production [15].

Both DLST and overall α-KGDHC are crucial in bioenergetic processes within mitochondria. In the central nervous system, the high metabolic demand can lead to a higher level of oxidative

stress via the production of free radicals. Under pathological conditions such as AD, oxidative stress can enhance the progression of the disease. To our knowledge, we are the first to demonstrate in vivo that the partial genetic deletion of mitochondrial DLST enzyme can accelerate the appearance of AD-like phenotype in a transgenic mouse model of amyloid deposition.

Supplementary Material

Refer to Web version on PubMed Central for supplementary material.

Acknowledgments

This work was supported by the National Institute of Health (NIH) grant 5P01 AG14930-08. We thank Huan-Lian Chen for his contribution in the breeding and genotyping of the $DLST^{+/-}$ mice, and both Saravanan Karuppagounder and Qingli Shi for providing scientific and technical support. We also thank Michael T. Lin for his inputs on the manuscript.

References

1. Canevari L, Abramov AY, Duchen MR. Toxicity of amyloid beta peptide: tales of calcium, mitochondria, and oxidative stress. Neurochem Res 2004;29:637–650. [PubMed: 15038611]
2. Smith MA, Hirai K, Hsiao K, Pappolla MA, Harris PL, Siedlak SL, Tabaton M, Perry G. Amyloid-beta deposition in Alzheimer transgenic mice is associated with oxidative stress. J Neurochem 1998;70:2212–2215. [PubMed: 9572310]
3. Butterfield DA, Drake J, Pocernich C, Castegna A. Evidence of oxidative damage in Alzheimer's disease brain: central role for amyloid beta-peptide. Trends Mol Med 2001;7:548–554. [PubMed: 11733217]
4. Butterfield DA, Lauderback CM. Lipid peroxidation and protein oxidation in Alzheimer's disease brain: potential causes and consequences involving amyloid beta-peptide-associated free radical oxidative stress. Free Radic. Biol. Med 2002;32:1050–1060. [PubMed: 12031889]
5. Smith MA, Richey Harris PL, Sayre LM, Beckman JS, Perry G. Widespread peroxynitrite-mediated damage in Alzheimer's disease. J Neurosci 1997;17:2653–2657. [PubMed: 9092586]
6. Butterfield DA, Reed TT, Perluigi M, De Marco C, Coccia R, Keller JN, Markesbery WR, Sultana R. Elevated levels of 3-nitrotyrosine in brain from subjects with amnestic mild cognitive impairment: implications for the role of nitration in the progression of Alzheimer's disease. Brain Res 2007;1148:243–248. [PubMed: 17395167]
7. Sayre LM, Zelasko DA, Harris PL, Perry G, Salomon RG, Smith MA. 4-Hydroxynonenal-derived advanced lipid peroxidation end products are increased in Alzheimer's disease. J Neurochem 1997;68:2092–2097. [PubMed: 9109537]
8. Ando Y, Brannstrom T, Uchida K, Nyhlin N, Nasman B, Suhr O, Yamashita T, Olsson T, El Salhy M, Uchino M, Ando M. Histochemical detection of 4-hydroxynonenal protein in Alzheimer amyloid. J Neurol Sci 1998;156:172–176. [PubMed: 9588853]
9. Nunomura A, Perry G, Aliev G, Hirai K, Takeda A, Balraj EK, Jones PK, Ghanbari H, Wataya T, Shimohama S, Chiba S, Atwood CS, Petersen RB, Smith MA. Oxidative damage is the earliest event in Alzheimer disease. J Neuropathol Exp Neurol 2001;60:759–767. [PubMed: 11487050]
10. Pratico D, Uryu K, Leight S, Trojanoswki JQ, Lee VM. Increased lipid peroxidation precedes amyloid plaque formation in an animal model of Alzheimer amyloidosis. J. Neurosci 2001;21:4183–4187. [PubMed: 11404403]
11. Abdul HM, Sultana R, St Clair DK, Markesbery WR, Butterfield DA. Oxidative damage in brain from human mutant APP/PS-1 double knock-in mice as a function of age. Free Radic Biol Med 2008;45:1420–1425. [PubMed: 18762245]
12. Li F, Calingasan NY, Yu F, Mauck WM, Toidze M, Almeida CG, Takahashi RH, Carlson GA, Flint Beal M, Lin MT, Gouras GK. Increased plaque burden in brains of APP mutant MnSOD heterozygous knockout mice. J. Neurochem 2004;89:1308–1312. [PubMed: 15147524]

13. Melov S, Adlard PA, Morten K, Johnson F, Golden TR, Hinerfeld D, Schilling B, Mavros C, Masters CL, Volitakis I, Li QX, Laughton K, Hubbard A, Cherny RA, Gibson B, Bush AI. Mitochondrial oxidative stress causes hyperphosphorylation of tau. PLoS ONE 2007;2:e536. [PubMed: 17579710]

14. Esposito L, Raber J, Kekonius L, Yan F, Yu GQ, Bien-Ly N, Puolivali J, Scearce-Levie K, Masliah E, Mucke L. Reduction in mitochondrial superoxide dismutase modulates Alzheimer's disease-like pathology and accelerates the onset of behavioral changes in human amyloid precursor protein transgenic mice. J. Neurosci 2006;26:5167–5179. [PubMed: 16687508]

15. Dumont M, Wille E, Stack C, Calingasan NY, Beal MF, Lin MT. Reduction of oxidative stress, amyloid deposition, and memory deficit by manganese superoxide dismutase overexpression in a transgenic mouse model of Alzheimer's disease. Faseb J. 2009

16. Gibson GE, Blass JP, Beal MF, Bunik V. The alpha-ketoglutarate-dehydrogenase complex: a mediator between mitochondria and oxidative stress in neurodegeneration. Mol Neurobiol 2005;31:43–63. [PubMed: 15953811]

17. Gibson GE, Sheu KF, Blass JP, Baker A, Carlson KC, Harding B, Perrino P. Reduced activities of thiamine-dependent enzymes in the brains and peripheral tissues of patients with Alzheimer's disease. Arch Neurol 1988;45:836–840. [PubMed: 3395256]

18. Butterworth RF, Besnard AM. Thiamine-dependent enzyme changes in temporal cortex of patients with Alzheimer's disease. Metab Brain Dis 1990;5:179–184. [PubMed: 2087217]

19. Mastrogiacomo F, Bergeron C, Kish SJ. Brain alpha-ketoglutarate dehydrogenase complex activity in Alzheimer's disease. J Neurochem 1993;61:2007–2014. [PubMed: 8245957]

20. Gibson GE, Zhang H, Sheu KF, Bogdanovich N, Lindsay JG, Lannfelt L, Vestling M, Cowburn RF. Alpha-ketoglutarate dehydrogenase in Alzheimer brains bearing the APP670/671 mutation. Ann Neurol 1998;44:676–681. [PubMed: 9778267]

21. Karuppagounder SS, Xu H, Shi Q, Chen LH, Pedrini S, Pechman D, Baker H, Beal MF, Gandy SE, Gibson GE. Thiamine deficiency induces oxidative stress and exacerbates the plaque pathology in Alzheimer's mouse model. Neurobiol Aging. 2008

22. Dumont M, Wille E, Calingasan NY, Tampellini D, Williams C, Gouras GK, Liby K, Sporn M, Nathan C, Flint Beal M, Lin MT. Triterpenoid CDDO-methylamide improves memory and decreases amyloid plaques in a transgenic mouse model of Alzheimer's disease. J Neurochem 2009;109:502–512. [PubMed: 19200343]

23. Chishti MA, Yang DS, Janus C, Phinney AL, Horne P, Pearson J, Strome R, Zuker N, Loukides J, French J, Turner S, Lozza G, Grilli M, Kunicki S, Morissette C, Paquette J, Gervais F, Bergeron C, Fraser PE, Carlson GA, George-Hyslop PS, Westaway D. Early-onset amyloid deposition and cognitive deficits in transgenic mice expressing a double mutant form of amyloid precursor protein 695. J. Biol. Chem 2001;276:21562–21570. [PubMed: 11279122]

24. Hirata-Fukae C, Li HF, Hoe HS, Gray AJ, Minami SS, Hamada K, Niikura T, Hua F, Tsukagoshi-Nagai H, Horikoshi-Sakuraba Y, Mughal M, Rebeck GW, LaFerla FM, Mattson MP, Iwata N, Saido TC, Klein WL, Duff KE, Aisen PS, Matsuoka Y. Females exhibit more extensive amyloid, but not tau, pathology in an Alzheimer transgenic model. Brain Res 2008;1216:92–103. [PubMed: 18486110]

25. Wang J, Tanila H, Puolivali J, Kadish I, van Groen T. Gender differences in the amount and deposition of amyloidbeta in APPswe and PS1 double transgenic mice. Neurobiol Dis 2003;14:318–327. [PubMed: 14678749]

26. Kayed R, Head E, Thompson JL, McIntire TM, Milton SC, Cotman CW, Glabe CG. Common structure of soluble amyloid oligomers implies common mechanism of pathogenesis. Science 2003;300:486–489. [PubMed: 12702875]

27. Hyde LA, Kazdoba TM, Grilli M, Lozza G, Brusa R, Zhang Q, Wong GT, McCool MF, Zhang L, Parker EM, Higgins GA. Age-progressing cognitive impairments and neuropathology in transgenic CRND8 mice. Behav. Brain Res 2005;160:344–355. [PubMed: 15863231]

28. Yoshiike Y, Minai R, Matsuo Y, Chen YR, Kimura T, Takashima A. Amyloid oligomer conformation in a group of natively folded proteins. PLoS ONE 2008;3:e3235. [PubMed: 18800165]

29. Placanica L, Zhu L, Li YM. Gender- and age-dependent gamma-secretase activity in mouse brain and its implication in sporadic Alzheimer disease. PLoS ONE 2009;4:e5088. [PubMed: 19352431]

30. Huang X, Atwood CS, Hartshorn MA, Multhaup G, Goldstein LE, Scarpa RC, Cuajungco MP, Gray DN, Lim J, Moir RD, Tanzi RE, Bush AI. The A beta peptide of Alzheimer's disease directly produces hydrogen peroxide through metal ion reduction. Biochemistry 1999;38:7609–7616. [PubMed: 10386999]

31. Varadarajan S, Yatin S, Kanski J, Jahanshahi F, Butterfield DA. Methionine residue 35 is important in amyloid beta-peptide-associated free radical oxidative stress. Brain Res Bull 1999;50:133–141. [PubMed: 10535332]

32. De Felice FG, Velasco PT, Lambert MP, Viola K, Fernandez SJ, Ferreira ST, Klein WL. Abeta oligomers induce neuronal oxidative stress through an N-methyl-D-aspartate receptor-dependent mechanism that is blocked by the Alzheimer drug memantine. J Biol Chem 2007;282:11590–11601. [PubMed: 17308309]

33. Keller JN, Kindy MS, Holtsberg FW, St Clair DK, Yen HC, Germeyer A, Steiner SM, Bruce-Keller AJ, Hutchins JB, Mattson MP. Mitochondrial manganese superoxide dismutase prevents neural apoptosis and reduces ischemic brain injury: suppression of peroxynitrite production, lipid peroxidation, and mitochondrial dysfunction. J Neurosci 1998;18:687–697. [PubMed: 9425011]

34. Shi Q, Chen HL, Xu H, Gibson GE. Reduction in the E2k subunit of the alpha-ketoglutarate dehydrogenase complex has effects independent of complex activity. J Biol Chem 2005;280:10888–10896. [PubMed: 15649899]

35. Ali SS, Xiong C, Lucero J, Behrens MM, Dugan LL, Quick KL. Gender differences in free radical homeostasis during aging: shorter-lived female C57BL6 mice have increased oxidative stress. Aging Cell 2006;5:565–574. [PubMed: 17129217]

36. Liu L, Komatsu H, Murray IV, Axelsen PH. Promotion of amyloid beta protein misfolding and fibrillogenesis by a lipid oxidation product. J. Mol. Biol 2008;377:1236–1250. [PubMed: 18304576]

37. Bieschke J, Zhang Q, Powers ET, Lerner RA, Kelly JW. Oxidative metabolites accelerate Alzheimer's amyloidogenesis by a two-step mechanism, eliminating the requirement for nucleation. Biochemistry 2005;44:4977–4983. [PubMed: 15794636]

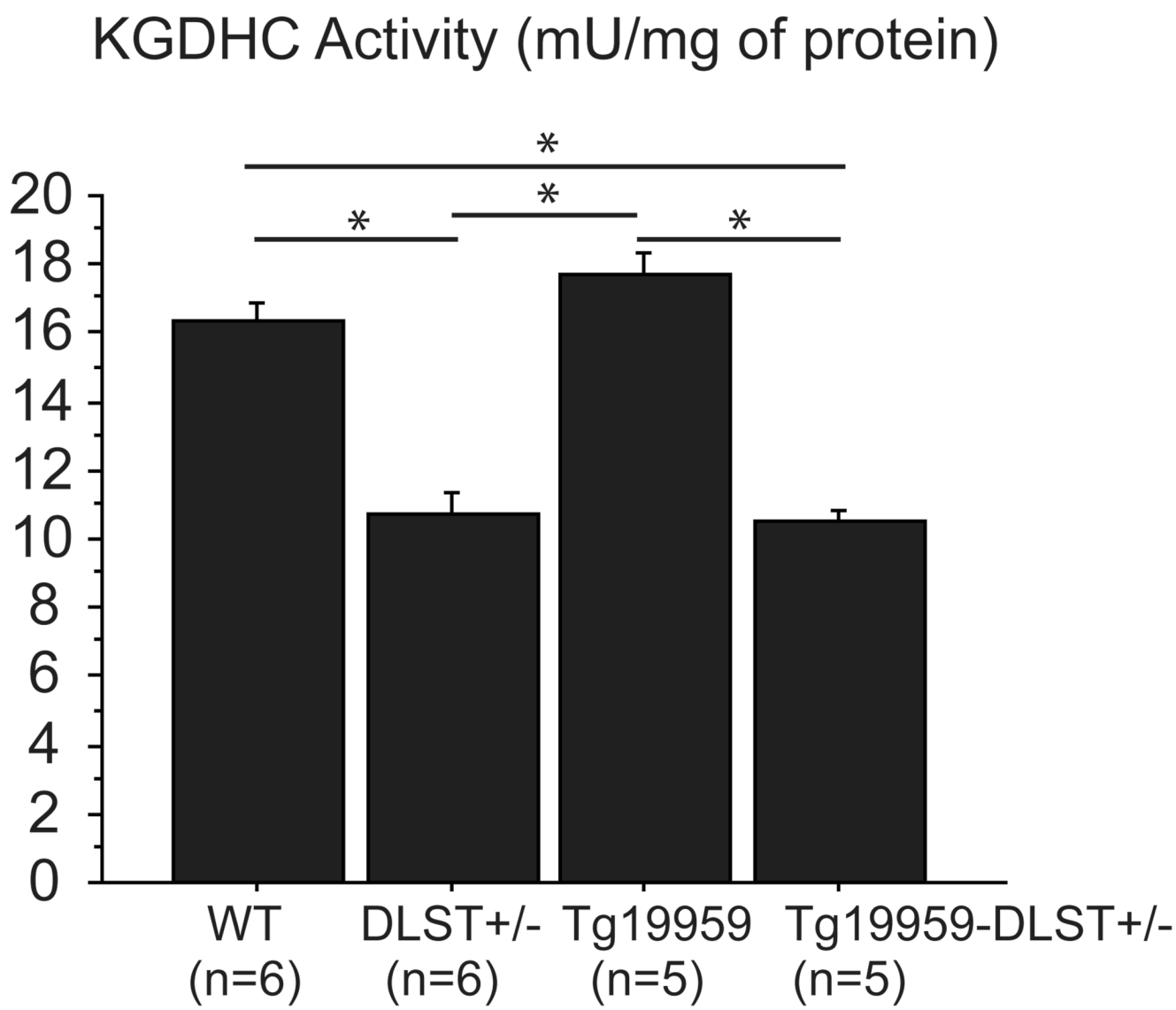

Figure 1. α-ketoglutarate dehydrogenase activity was reduced in Tg19959 mice with DLST deficiency

Measurement of α-KGDHC activity per mU/mg of protein in wild-type, DLST$^{+/-}$, Tg19959 mice and Tg19959-DLST$^{+/-}$ littermates. Data are expressed as means ± standard errors. KGHDC activity was reduced in DLST$^{+/-}$ and Tg19959-DLST$^{+/-}$ mice compared to wild-type and Tg19959 littermates (* $p<0.05$).

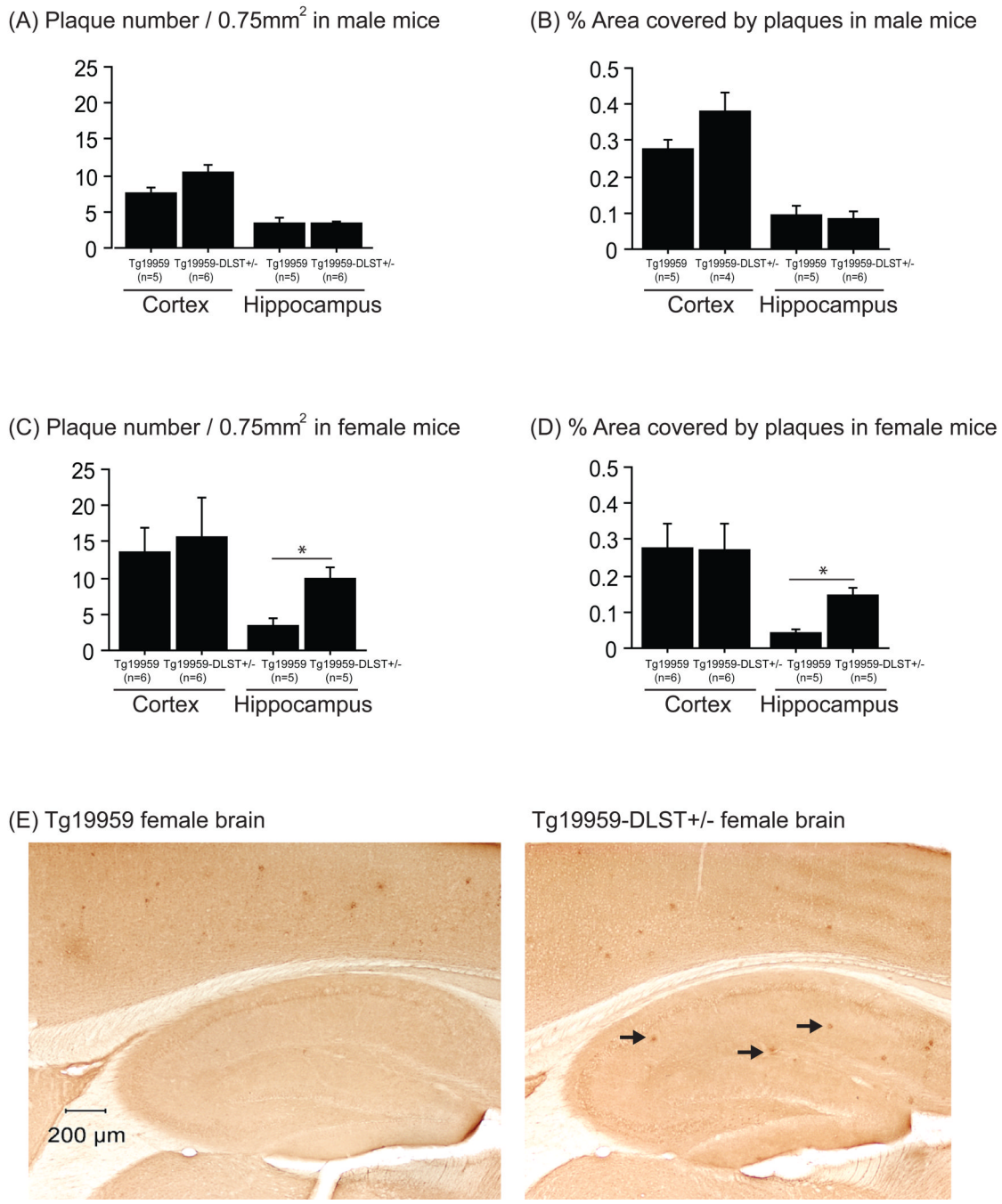

Figure 2. DLST deficiency increased amyloid plaque burden in female Tg19959 mice

Amyloid plaque number (A for males and C for females) and percent area covered by amyloid plaques (B for males and D for females) in the cortex and the hippocampus of Tg19959 mice and Tg19959-DLST$^{+/-}$ littermates. Data are expressed as means ± standard errors. (E) Photographs of female brain sections labeled with AB5078P antibody to visualize Aβ deposits (black arrows). DLST deficiency increased hippocampal amyloid deposition in female Tg19959 mice (* $p<0.05$).

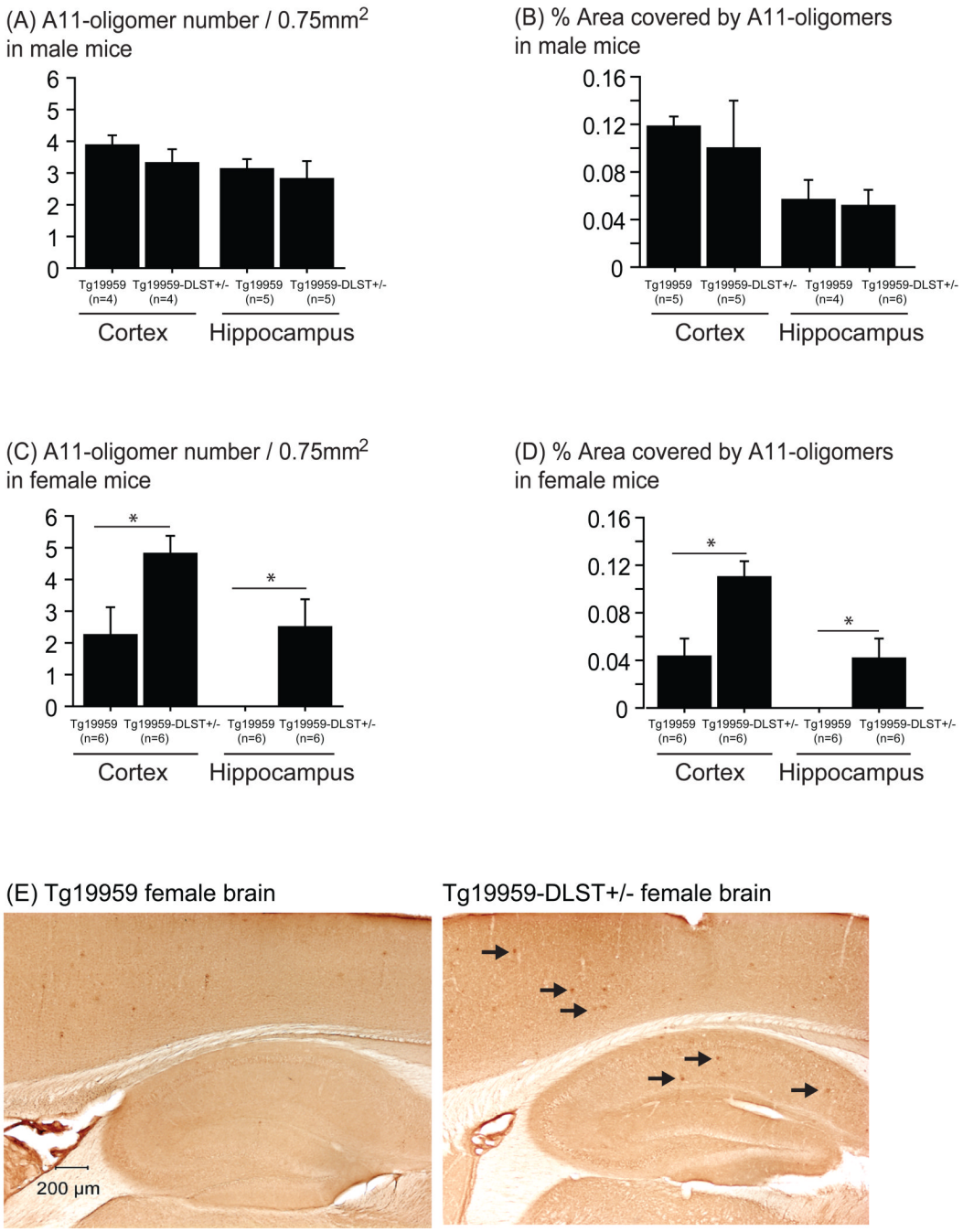

Figure 3. DLST deficiency increased Aβ oligomers in female Tg19959 mice

A11 oligomer number (A for males, C for females) and percent area covered by A11 oligomers (B for males, D females) in the cortex and the hippocampus of Tg19959 mice and Tg19959-DLST$^{+/-}$ littermates. Data are expressed as means ± standard errors. (E) Photographs of female brain sections labeled with A11 antibody to visualize Aβ oligomers (black arrows). DLST deficiency increased Aβ oligomers in the cortex and the hippocampus of female Tg19959 mice (* $p<0.05$).

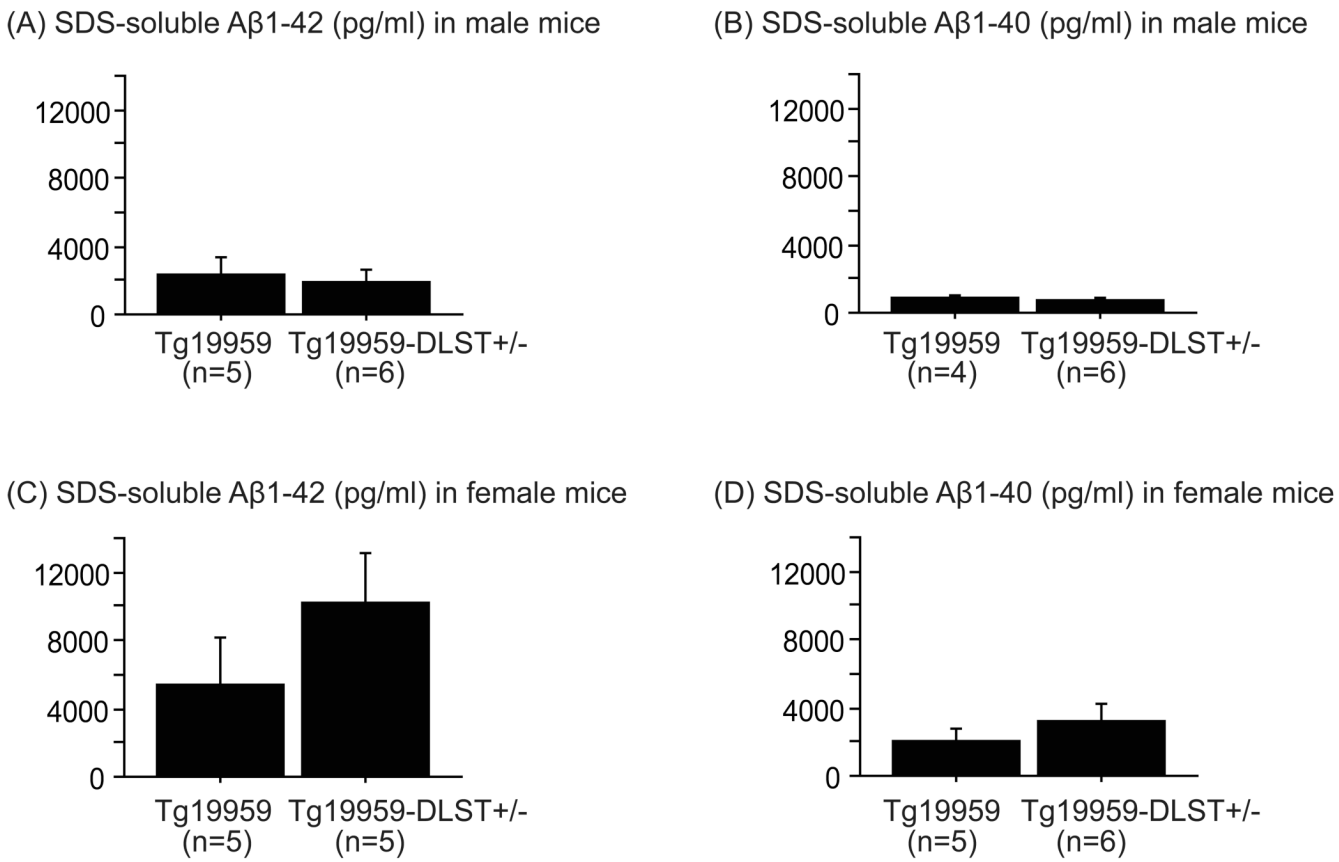

Figure 4. DLST deficiency did not affect levels of SDS-soluble Aβ1–42 and Aβ1–40 in Tg19959 mice

Quantification of 6% SDS-soluble Aβ1–42 (A for males and C for females) and 6% SDS-soluble Aβ1–40 (B for males and D for females) levels by ELISA in Tg19959 mice and Tg19959-DLST$^{+/-}$ littermates. Data are expressed as means ± standard errors. DLST deficiency did not change levels of SDS-soluble Aβ1–42 and Aβ1–40 in Tg19959 mice.

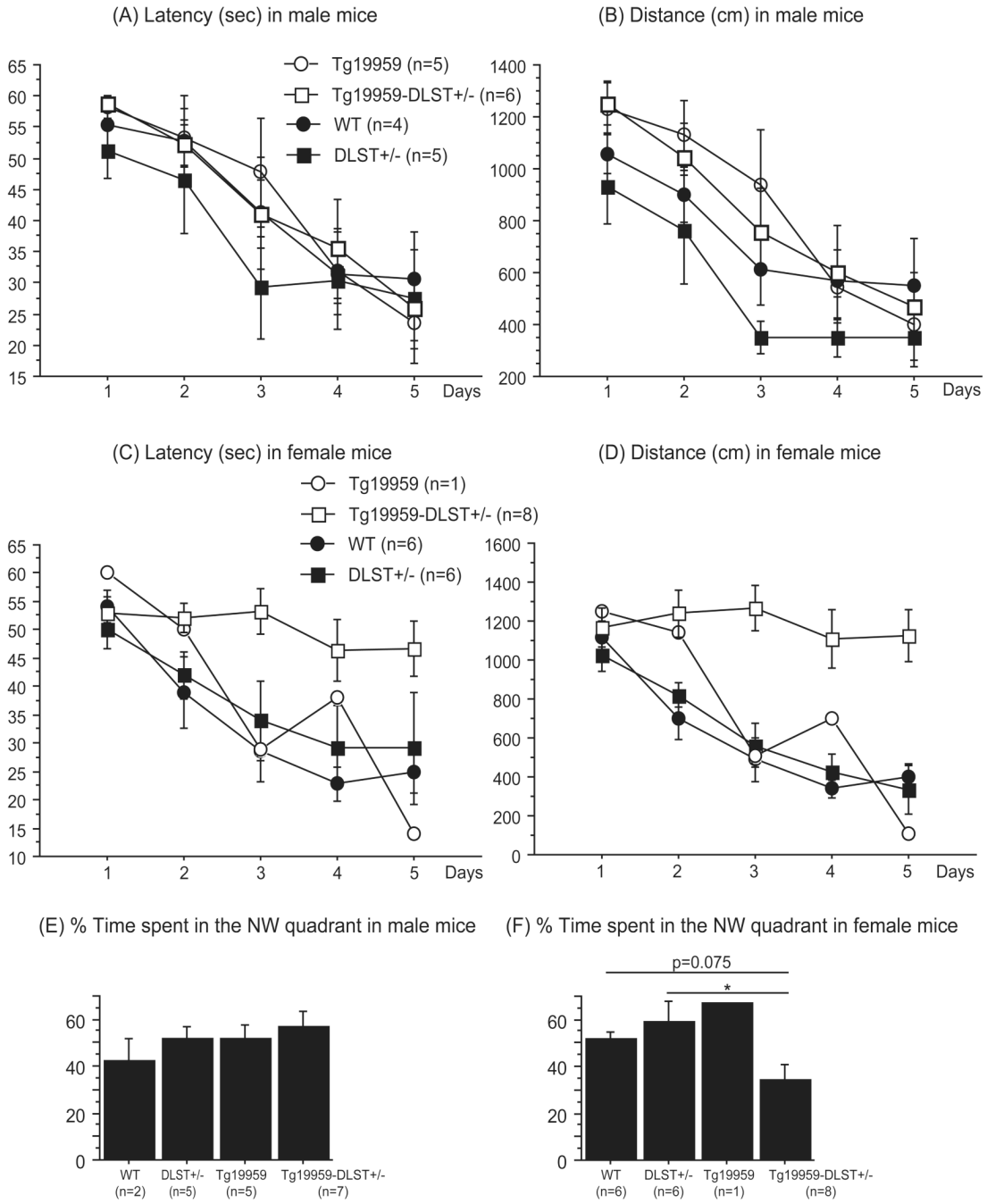

Figure 5. DLST deficiency induced spatial learning and memory impairment in female Tg19959 mice

Latencies (A for males and C for females) and distances (B for males and D for females) before reaching the hidden platform during the acquisition period in wild-type, DLST$^{+/-}$, Tg19959 mice and Tg19959-DLST$^{+/-}$ littermates. Data are expressed as means ± standard errors. DLST deficiency induced spatial learning deficit in female Tg19959 mice, as shown by the increased distance traveled during the acquisition period, especially on the last day of training (* $p<0.05$). Percent time spent in the NW quadrant during the probe trial (E for males and F for females) in wild-type, DLST$^{+/-}$, Tg19959 mice and Tg19959-DLST$^{+/-}$ littermates. Data are expressed as means ± standard errors. DLST deficiency induced spatial memory impairment in female

Tg19959 mice, as shown by the decreased percent time spent in the NW quadrant of the pool (* $p<0.05$).

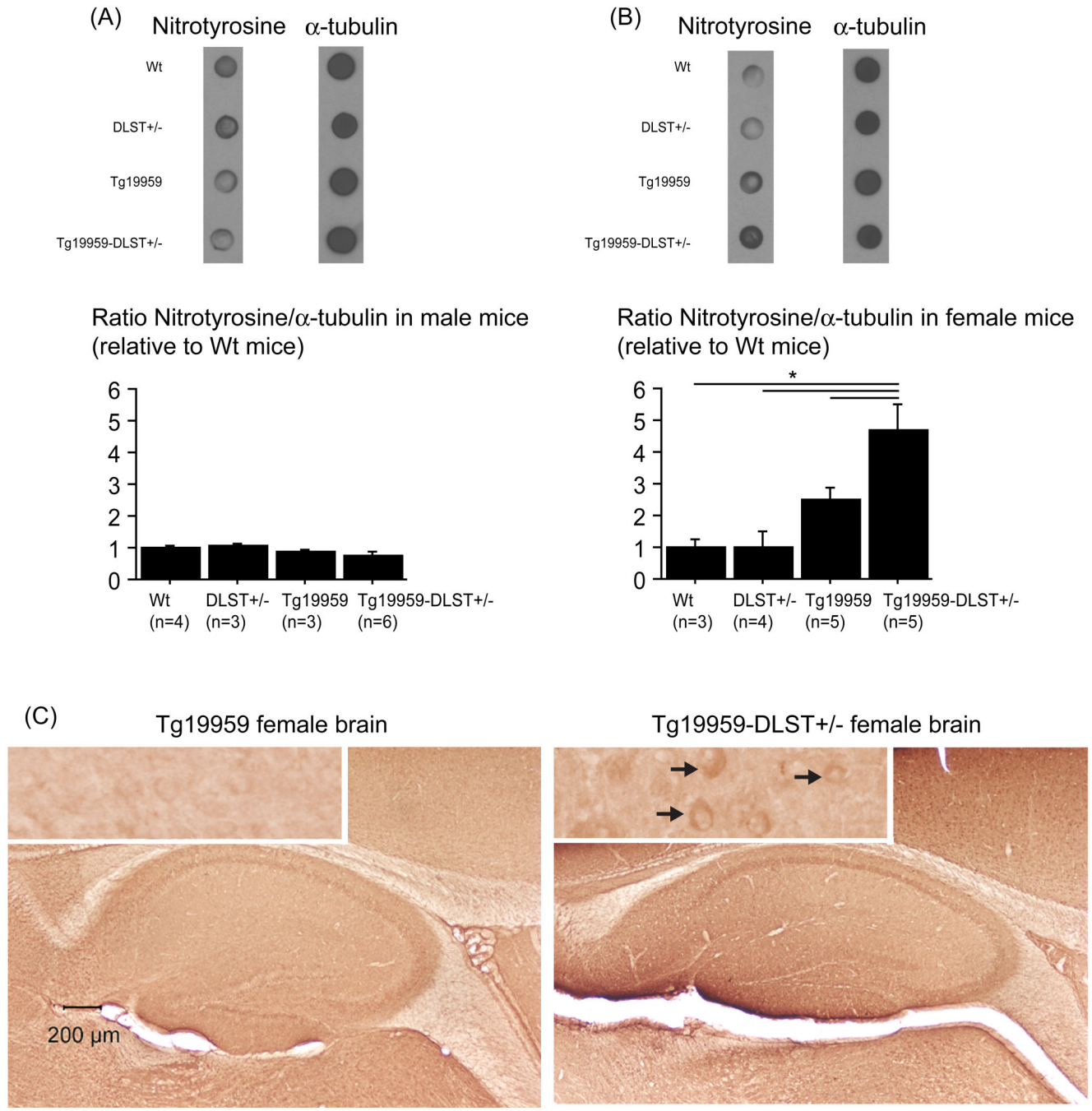

Figure 6. DLST deficiency increased nitrotyrosine levels in female Tg19959 mice

Dot-blot of nitrotyrosine in male (A) and female mice (B). Data are expressed as ratios of nitrotyrosine to tubulin relative to wild-type mice (means ± standard errors). (C) Photographs of female brain sections labeled with anti-nitrotyrosine antibody (black arrows), including a high magnification of the cortex. In Tg19959-DLST$^{+/-}$ female mice, level of nitrotyrosine was increased compared to wild-type, DLST$^{+/-}$ and Tg19959 female littermates (* $p<0.05$).